



Steering electron correlation time by elliptically polarized femtosecond laser pulses

HUIPENG KANG,^{1,2} YUEMING ZHOU,^{3*} AND PEIXIANG LU^{3,4}

¹*Institut für Kernphysik, Goethe Universität Frankfurt, 60438 Frankfurt am Main, Germany*

²*State Key Laboratory of Magnetic Resonance and Atomic and Molecular Physics, Wuhan Institute of Physics and Mathematics, Chinese Academy of Sciences, Wuhan 430071, China*

³*School of Physics, Huazhong University of Science and Technology, Wuhan 430074, China*

⁴*Laboratory of Optical Information Technology, Wuhan Institute of Technology, Wuhan 430205, China*
**zhouymhust@hust.edu.cn*

Abstract: Electron correlation is ubiquitous across diverse physical systems from atoms and molecules to condensed matter. Observing and controlling dynamical electron correlation in photoinduced processes paves the way to the coherent control of chemical reactions and photobiological processes. Here, we experimentally investigate dynamics of electron correlation in double ionization of neon irradiated by intense elliptically polarized laser pulses. We find a characteristic, ellipticity-dependent, correlated electron emission along the minor axis of the elliptically polarized light. This observation is well reproduced by a semi-classical ensemble model simulation. By tracing back the corresponding electron trajectories, we find that the dynamical energy sharing during the electron emission process is modified by the ellipticity of the laser light. Thus, our work provides evidence for a possible ultrafast control of the energy sharing between the correlated electrons by varying the light ellipticity.

© 2018 Optical Society of America under the terms of the [OSA Open Access Publishing Agreement](#)

1. Introduction

Electron correlation plays an essential role in many important processes such as superconductivity and chemical reaction in modern physics and chemistry. In ultrafast laser science, multiphoton non-sequential double ionization (NSDI) is a fundamental and important process relying completely on electron correlation. It has continued to receive intense experimental and theoretical attention (for reviews, see [1,2]). This phenomenon manifests itself as an enhancement of the double ionization yield by orders-of-magnitude over the yield one would expect for the sequential and independent removal of electrons in the absence of electron correlation. Over a range of intermediate laser intensities NSDI has been discovered in all rare gas atoms [3] and some molecules [4–8]. During the past two decades, numerous studies on NSDI have continuously deepened our understanding of strong field electron correlation. Kinematically complete experiments [9–12] have provided convincing evidences that the well-known recollision [13] is the dominant mechanism driving NSDI. In this process, after tunneling through the distorted Coulomb potential, the first emitted electron may be accelerated and driven back to its parent ion by the oscillating laser field, where it can kick out a second electron through inelastic scattering.

According to the recollision scenario, the correlated behavior of the two electrons depends strongly on the laser intensity. At low intensities, the energy of the returning electron is not sufficient to free the second electron. Instead the second electron can be lifted to an excited state by the recollision process in a first step and afterwards be ionized (in a second step) by the laser field. This process has been named recollision excitation with subsequent ionization (RESI). At high intensities, the return electron acquires a large amount of energy from the laser field and it can directly ionize the second electron during the recollision. The latter process is referred to as recollision-impact ionization (RII). Depending on whether the double ionization proceeds via the RII or the RESI pathway, the correlated electron momentum distribution along the polarization

direction of the laser field may exhibit correlation [10, 11] or an anticorrelation pattern [14].

A striking difference between RESI and RII is the time lag between recollision and double ionization. For the RESI pathway, the excited electron usually ionizes around the first maximum of the electric field after the recollision. Because the highest energy recollision occurs around the field zero-crossing, this leads to a time delay of around $T/4$ (T is the optical cycle of the laser field) between double ionization and recollision. The observation of anti-correlation patterns in double electron emission spectra [14] provides experimental evidence supporting this time delay. On the other side, for the RII pathway, it is unclear whether double ionization occurs immediately or after a short time delay after recollision. Some theoretical calculations [15–17] have shown that there might exist a time delay lasting for a small fraction of T . It can be interpreted as the time required for the dynamic energy sharing mediated by the electron-electron interaction during the recollision [17]. A related scenario was discussed by Liu *et al.* who argued that the energy deposited in the recollision can be thermalized in a multielectron target before a second electron is ejected [15, 16].

In this paper, we analyze fully differential measurements on double ionization of neon by elliptically polarized femtosecond laser pulses. Using a semi-classical model we find that the measured correlated electron momentum distributions along the minor axis of elliptical polarization are sensitive to the probability distribution of the time delay between recollision and double ionization. By varying the ellipticity, the ratio of recolliding electron trajectories with time delay <135 as and >135 as changes, giving rise to the observed ellipticity-dependent electron emission into different quadrants of the correlated electron spectra. Our work presents experimental evidences of the existence of short time delay of several hundred attoseconds in RII-dominant double ionization, and further provides insight into how to control the energy exchange between the correlated electrons on a sub-femtosecond scale by varying the ellipticity.

2. Experimental setup

We adopted a Cold Target Recoil Ion Momentum Spectroscopy (COLTRIMS) reaction microscope [18] to measure the three-dimensional momentum distributions of the doubly charged Ne ion and one of the emitted electrons in coincidence. A commercial Ti:Sapphire femtosecond laser system (788 nm, 100 kHz, 100 μ J, 45 fs, Wyvern-500, KMLabs) was used to produce intense laser pulses. We adopted a quarter-wave plate to generate the elliptically polarized light which has been used for ionizing a cold supersonic neon gas jet in the chamber. The photoelectrons and photoions were accelerated by homogeneous electric (23.0 V/cm) and magnetic (9.2 G) fields towards two microchannel plate detectors equipped with delay-line anodes [19] for position readout. The spectrometer consisted of an ion arm with an 18.2 cm acceleration region and a 40.0 cm drift region, and an electron arm with an acceleration region of 7.8 cm. The three-dimensional momenta of the photoelectrons and photoions can be retrieved from their impact positions on the detectors and the times of flight. To avoid dead-time problems of the electron detector, we measured the momenta of one of the double emitted electrons and the doubly charged ion. The other electron's momentum was deduced via momentum conservation. Other aspects from the same measurement campaign have been reported in [20, 21]. The laser peak intensity was calibrated by measuring the “donut”-shape electron momentum distribution from single ionization of Ne using circularly polarized light [22]. The uncertainty of the peak intensity was estimated to be $\pm 20\%$.

3. Theoretical model

Theoretically, quantum calculations, such as the numerical solution of time-dependent Schrödinger equation for two electrons, are enormously demanding concerning computational resources and have therefore been confined to certain NSDI cases [23, 24]. In the past decades, numerous studies of NSDI have resorted to semi-classical or classical ensemble models [25, 26]. It has been shown

that these models are very successful not only in reproducing the experimental features [27, 28] but also in predicting new phenomena [29, 30], and they are capable of offering an intuitive picture of the underlying mechanism. Here, we employ the widely used semi-classical ensemble model to describe strong field double ionization of Ne with elliptically polarized laser pulses.

In the semi-classical model, the first electron is ionized through tunneling with a probability given by tunneling theory [31]. This tunneled electron is placed at the tunneling exit with zero initial parallel momentum and a Gaussian distribution of transverse momentum [32]. The initial condition of the second electron is modeled by a microcanonical ensemble with the energy of -1.5 a.u., i.e., the second ionization potential of Ne [27, 30]. After the tunneling ionization of the first electron, the evolution of the two-electron system in two dimensions is described by the classical Newtonian equation (atomic units are used throughout this paper)

$$\frac{d^2 \mathbf{r}_i}{dt^2} = -\mathbf{E}(t) - \nabla(V_{ne}^i + V_{ee}), \quad (1)$$

where $\mathbf{E}(t) = (E_y(t), E_z(t))$ is the electric field of the elliptically polarized laser pulse with $E_y(t) = \epsilon E_{0y} f(t) \sin \omega t$ and $E_z(t) = E_{0z} f(t) \cos \omega t$. Here ω is the laser frequency, ϵ is the ellipticity of the laser pulses, and $f(t)$ is the envelope of the pulses which have a constant amplitude for the first eight cycles and then linearly turns off during two cycles. $V_{ne}^i = -\frac{2}{\sqrt{r_i^2 + a^2}}$ and $V_{ee} = \frac{1}{\sqrt{(r_1 - r_2)^2 + b^2}}$ are the nucleus-electron and electron-electron interaction potentials, respectively. The screening parameters $a = 0.5$ and $b = 0.01$ are chosen to avoid the singularity of Coulomb potential in the simulations [30]. For simplicity, we restricted the motion of the electrons to the laser polarization plane. The evolution of the two-electron system is traced until the end of the laser pulse according to Eq. (1). The double ionization event is identified when the energies of both electrons are positive after the laser pulse is turned off. The ensemble sizes in our simulations are as large as several millions which result in more than 10^4 double ionization events at the end of the pulses for statistic.

Note that in the semi-classical model, the second electron could be excited to the states with energy lower than the first excited state of Ne^+ through the recollision. In order to eliminate this unphysical process, we have abandoned such double ionization events in our calculation.

4. Results and discussion

For the double ionization by elliptically polarized light, most previous investigations theoretically studied the correlated electron momentum spectra along the major axis of the polarization ellipse [33–35]. Only a little attention has been paid to the correlated electron dynamic along the minor axis, so far [20]. In Figs. 1(a1)~1(a4) we display the correlated electron momentum distributions in the y -direction (the minor axis of elliptical polarization) recorded at a peak intensity of 5×10^{14} W/cm² for light ellipticities ranging from 0 to 0.25. Under these experimental conditions, we have previously shown that the Ne double ionization mainly occurs via the RII pathway [20, 21]. The data show that, when the ellipticity is increased above 0.18, the distributions show an increasing fraction of events in the first and third quadrants [Figs. 1(a3) and 1(a4)]. This feature is well captured by the semi-classical ensemble calculation in Figs. 1(b1)~1(b4). The discrepancy in the momentum values for each ellipticity possibly results from the fact that the actual peak intensity in experiments could be lower than the one used in the calculation (i.e. there is a $\pm 20\%$ uncertainty of the peak intensity calibration in our experiment).

The electron pairs in the first and third quadrants indicate a side-by-side emission along the y -axis. While the electron pairs in the second and fourth quadrants represent a back-to-back emission. In order to retrieve quantitative information about the electron emissions into different

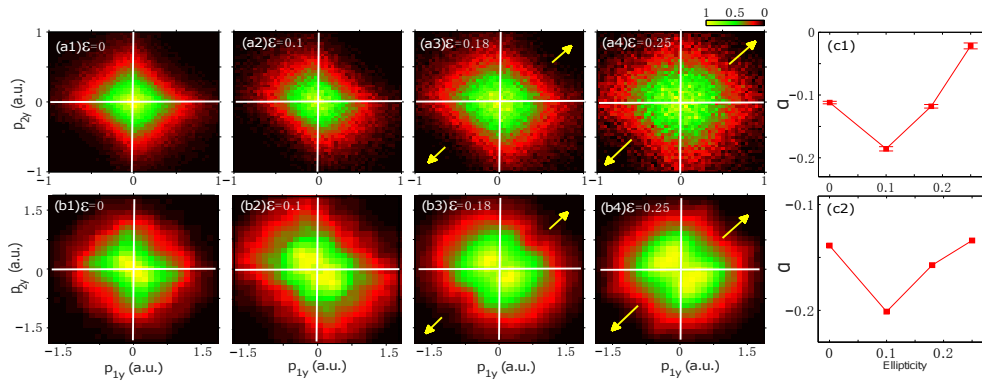


Fig. 1. Experimental (a1)~(a4) and calculated (b1)~(b4) correlated electron momentum distributions along the minor axis of elliptical polarization (i.e., the y -axis) with ellipticities in a range from 0 to 0.25, at a peak intensity of 5×10^{14} W/cm² and a central wavelength of 788 nm. The color scales have been normalized for comparison purposes. The yellow arrows in (a3), (a4), (b3), and (b4) indicate the directions where the electron distributions are expanded. (c1) and (c2) Experimental extracted and calculated asymmetry parameter for various ellipticities, respectively. The error bars in (c1) show statistical errors.

directions, we introduce an asymmetry parameter:

$$\alpha = \frac{Y_{1+3} - Y_{2+4}}{Y_{1+3} + Y_{2+4}}, \quad (2)$$

where Y_{1+3} and Y_{2+4} represent the integrated yields in the first and third quadrants and in the second and fourth quadrants, respectively. This parameter reflects the asymmetry between the side-by-side and back-to-back emission. A smaller value corresponds to more back-to-back emission. The experimentally extracted and the calculated asymmetry parameters for various ellipticities are shown in Figs. 1(c1) and 1(c2), respectively. One can see that the experimental parameter first decreases when the ellipticity goes to $\epsilon = 0.1$ and then increases with further increasing ellipticities. This interesting feature is well reproduced by our calculation. The discrepancy in the values of asymmetry parameter is partially due to the overestimated electron repulsion effect in our two-dimensional model calculation.

To gain insight into the origin of our observations, we first perform a statistical analysis on the time delay t_d between double ionization and recollision for various ellipticities, as shown in Fig. 2(a). This time delay in the RII dominant double ionization represents the time required sharing the energy between the two correlated electrons upon recollision, and it has been theoretically investigated for linear laser polarization very recently [17]. Here the recollision time is defined as the time of closest approach of the two electrons after tunneling, and the double ionization time is defined as the instant when both electrons achieve positive energies, where each electron energy is calculated considering the kinetic energy, potential energy of the electron-ion interaction and half of electron-electron repulsive energy [17, 36]. The calculations show two peaks $t_d \sim 0$ and $t_d \sim 0.12T$ (~ 324 as) for every ellipticity. An obvious dependence of the relative peak height on the ellipticity can be seen.

According to the calculation, the double ionization events can be conveniently separated into two cases I and II, i.e., $t_d < 0.05T$ (~ 135 as) and $t_d > 0.05T$, respectively. For case I the two electrons are almost simultaneously released into the laser field. The Coulomb repulsion between them is strong and thus the back-to-back final emission is more favorable. Whereas for case II there is a remarkable time delay around $0.12T$ (~ 324 as) between the release times of the two electrons. The e-e repulsion effect becomes weak and thus the back-to-back final

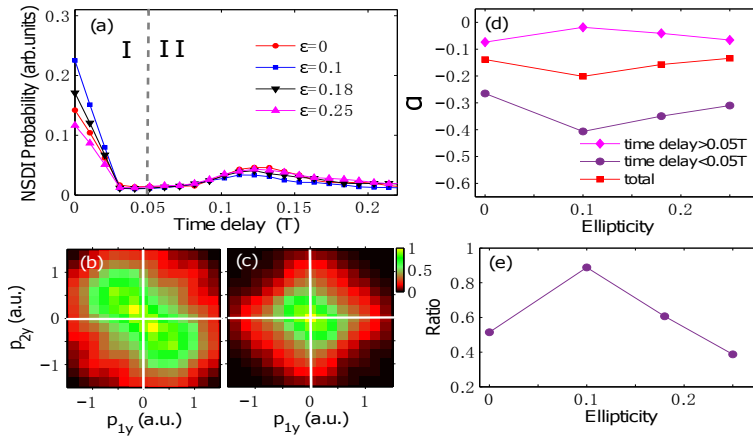


Fig. 2. (a) Probability distributions of the time delay t_d between recollision and double ionization for various ellipticities. The results have been normalized so that the integrated areas of different curves are the same for comparison purposes. (b) Calculated correlated electron momentum distribution along the y direction at the ellipticity $\epsilon = 0.1$. Here, only the double ionization event with $t_d < 0.05T$ are included, corresponding to case I in (a). (c) The same as (b) but for the double ionization events with $t_d > 0.05T$, corresponding to case II in (a). The color scales have been normalized for comparison purposes. (d) The asymmetry parameters for different ellipticities. Here, we have calculated the asymmetry parameters for the double ionization events with $t_d < 0.05T$ (circles) and $t_d > 0.05T$ (diamonds), respectively. The red squares represent the asymmetry parameter for the total double ionization events, which is the same as in Fig. 1(c2). (e) The ratio between the events with $t_d < 0.05T$ and that with $t_d > 0.05T$ for different ellipticities.

emission is suppressed. This is a good approximation for small ellipticities $\epsilon \leq 0.1$, where the y -component of the laser field has a negligible effect on the electrons. The difference between case I and II is highlighted in Figs. 2(b) and 2(c), where we compare the calculated correlated electron momentum spectrum for $t_d < 0.05T$ and that for $t_d > 0.05T$ at the ellipticity of 0.1. The electron pairs are much more likely to distribute in the second and fourth quadrants for $t_d < 0.05T$. Additionally, the electron momenta in these two quadrants extend to much larger values, suggesting a stronger Coulomb repulsion between the two electrons at their release times.

In Fig. 2(d) we further show the calculated asymmetry parameter for double ionization events with $t_d < 0.05T$ and $t_d > 0.05T$, respectively. For every ellipticity, the asymmetry parameter for $t_d < 0.05T$ is always smaller than that for $t_d > 0.05T$. The value of the total asymmetry parameter is related to the ratio between the double ionization events with $t_d < 0.05T$ and that with $t_d > 0.05T$. Therefore, the probability distribution of t_d leaves its footprint in the asymmetry parameter. In Fig. 2(e) we present the calculated ratio between double ionization events with $t_d < 0.05T$ and that with $t_d > 0.05T$ for various ellipticities. This clearly shows that, with increasing ellipticity, the ratio first increases and then decreases, leading to the observed ellipticity-dependent asymmetry parameter in Fig. 1(c1). Our observation and analysis indicate on one hand, that the correlated electrons' energy sharing process is modified by the elliptical polarization and becomes slower for higher ellipticities. This implies on the other hand, that this e-e energy sharing process could be steered on a sub-femtosecond scale by varying the ellipticity.

The ellipticity-dependent ratio in Fig. 2(e) is closely related to the distinct behaviors of recollisional trajectories for different ellipticities. The contributions to recollision-induced double ionization can be distinguished into single-return-collision (SRC) and multiple-return-collision

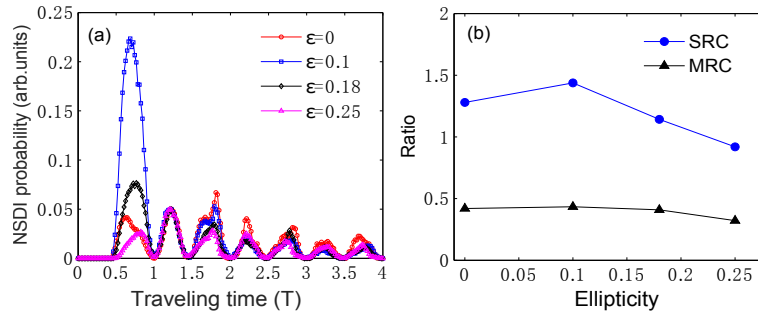


Fig. 3. (a) Probability distributions of the electron traveling time (the time lag between recollision and tunneling ionization of the first electron) for different ellipticities. Here, the curves have been normalized so that the height of peak at $1.25T$ is the same for comparison purposes. (b) The ratio of the double ionization events with $t_d < 0.05T$ and that with $t_d > 0.05T$. Here, we separately show the results for the SRC (blue circles) and MRC (black triangles) trajectories, respectively.

(MRC) trajectories, depending upon whether the recollision occurs when the tunnel-ionized electron returns to the ion for the first time or after passing the ion at least once [37]. It has been demonstrated that the relative contributions of SRC (or MRC) trajectories depend critically on the ellipticity [34]. In Fig. 3(a) we show the calculated probability distributions of electron travel time for various ellipticities. The first peak corresponds to the SRC trajectories and the following peaks represent the MRC trajectories. As can be seen, the relative contributions of SRC first increase and then decrease with increasing ellipticities, which is in good agreement with previous studies [20, 34]. To show how this is related to the evolution of the ratio in Fig. 2(e), we separately calculate this ratio for the SRC and MRC trajectories in Fig. 3(b). The results show that for SRC trajectories, the ratio ranges from 1 to 1.5. For the MRC trajectories, the ratio decreases to only about 0.4. This is closely related to the different recollision energy distributions for the SRC and MRC trajectories. This energy has larger distributions for the SRC trajectories and thus the second electron is expected to be ionized more quickly upon the first recollision, which tends to result in a short time delay. Consequently, the dependence of the SRC and MRC trajectories on the ellipticity results in the evolution of the ratio between double ionization events with $t_d < 0.05T$ and that with $t_d > 0.05T$. This means that the e-e energy sharing process is adjusted through steering the different recollisional trajectories by varying the ellipticity.

In the discussions above, we have ignored the effect of the laser field in the y direction on the correlated electron emissions, which is a good approximation for small ellipticities $\epsilon \leq 0.1$. Note that the y -component of the laser field is fully considered in our calculations above. As the ellipticity is increased, the y -component of the laser field plays a significant role for the final y -component of the electron momenta from double ionization events with $t_d > 0.05T$ where the e-e repulsive effect is suppressed. Whereas for the events with $t_d < 0.05T$, the laser field still plays a minor role due to the strong e-e repulsive effect therein. To show this more clearly, in Fig. 4 we display the calculated asymmetry parameters for the double ionization events with $t_d < 0.05T$ and that with $t_d > 0.05T$. Here laser field along the y direction has been switched off since the double ionization instant in the calculations. The results from calculations with inclusion of the laser field [red squares in Fig. 2(d)] are also shown here for comparison purposes. One can find that, for the ellipticity of 0.1, the results for both events are very similar to those from the full calculations, which confirms that the y -component field has no obvious effects on the electron emissions here. For higher ellipticities $\epsilon \geq 0.18$, however, the values of α for $t_d > 0.05T$ are significantly increased when considering the laser field. Meanwhile, no obvious changes of α for $t_d < 0.05T$ can be seen. This reveals the important effect of the y -component of

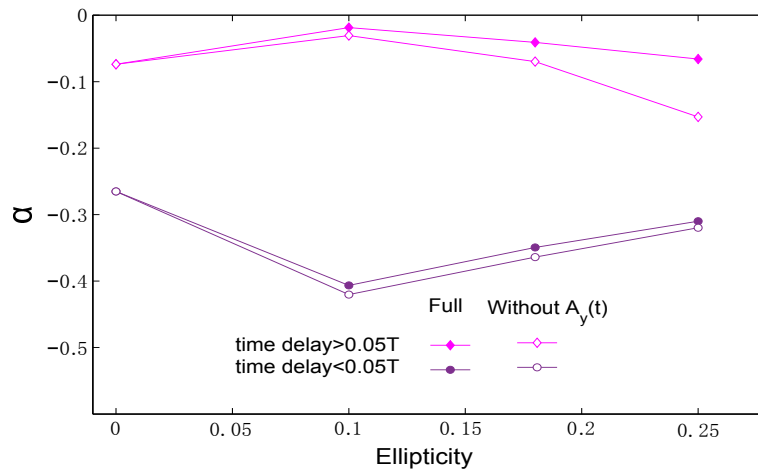


Fig. 4. The asymmetry parameter α for various ellipticities. The empty symbols indicate the calculations with the laser field turned off after the double ionization instant. The solid symbols indicate the full calculations, which are the same as Fig. 2(d). We separately show α for the double ionization events with $t_d < 0.05T$ (circles) and $t_d > 0.05T$ (diamonds), respectively.

the laser field for the double ionization events with $t_d > 0.05T$ for higher ellipticities: it tends to lead to side-by-side emissions here. This is because the two correlated electrons are drifted by the laser field in the same y direction for such ellipticities [20].

5. Conclusion

In conclusion, we experimentally investigate the double ionization of neon in intense elliptically polarized laser fields. A novel ellipticity-dependent correlated electron emission along the minor axis of polarization is observed. By employing a semi-classical model, our observations can be attributed to the characteristic ellipticity-dependent probability distributions of the time delay between recollision and double ionization. This time delay - lasting for several hundred attoseconds - represents the time which is required for sharing the energy between the correlated electrons upon recollision. This implies that the first electron is not far away from the second electron right after the recollision and the energy sharing between the two electrons can not be completely ignored for a while. Our work demonstrates that the details of this e-e energy sharing process depend distinctly on the exact parameters of the elliptical polarization, thus providing insight into how to control this process on a sub-femtosecond scale.

Funding

National Natural Science Foundation of China (NNSFC) (11622431, 61475055).

Acknowledgments

We thank Xiaolei Hao for valuable discussions. Huipeng Kang acknowledges support by the Alexander von Humboldt Foundation.

References

1. R. Dörner, Th. Weber, M. Weckenbrock, A. Staudte, M. Hattass, H. Schmidt-Böcking, R. Moshhammer, and J. Ullrich, "Multiple Ionization in Strong Laser Fields," *Adv. At. Mol. Opt. Phys.* **48**, 1-34 (2002).

2. W. Becker, X. Liu, P. Ho, and J. H. Eberly, "Theories of photoelectron correlation in laser-driven multiple atomic ionization," *Rev. Mod. Phys.* **84**, 1011-1043 (2012).
3. A. l'Huillier, L.A. Lompre, G. Mainfray, and C. Manus, "Multiply charged ions induced by multiphoton absorption in rare gases at 0.53 μm ," *Phys. Rev. A* **27**, 2503-2512 (1983).
4. C. Guo, M. Li, J.P. Nibarger, and G.N. Gibson, "Single and double ionization of diatomic molecules in strong laser fields," *Phys. Rev. A* **58**, R4271-R4274 (1998).
5. C. Cornaggia and Ph. Hering, "Nonsequential double ionization of small molecules induced by a femtosecond laser field," *Phys. Rev. A* **62**, 023403 (2000).
6. A. S. Alnaser, T. Osipov, E. P. Benis, A. Wech, B. Shan, C. L. Cocke, X. M. Tong, and C. D. Lin, "Rescattering Double Ionization of D_2 and H_2 by Intense Laser Pulses," *Phys. Rev. Lett.* **91**, 163002 (2003).
7. E. Eremina, X. Liu, H. Rottke, W. Sandner, M. G. SchÄdtzel, A. Dreischuh, G. G. Paulus, H. Walther, R. Moshhammer, and J. Ullrich, "Influence of Molecular Structure on Double Ionization of N_2 and O_2 by High Intensity Ultrashort Laser Pulses," *Phys. Rev. Lett.* **92**, 173001 (2004).
8. L. He, P. Lan, A. Le, B. Wang, B. Wang, X. Zhu, P. Lu, and C. D. Lin, "Real-Time Observation of Molecular Spinning with Angular High-Harmonic Spectroscopy," *Phys. Rev. Lett.* **121**, 163201 (2018).
9. Th. Weber, H. Giessen, M. Weckenbrock, G. Urbasch, A. Staudte, L. Spielberger, O. Jagutzki, V. Mergel, M. Vollmer, and R. Dörner, "Correlated electron emission in multiphoton double ionization," *Nature* **405**, 658-661 (2000).
10. Th. Weber, M. Weckenbrock, A. Staudte, L. Spielberger, O. Jagutzki, V. Mergel, F. Afaneh, G. Urbasch, M. Vollmer, H. Giessen, and R. Dörner, "Recoil-Ion Momentum Distributions for Single and Double Ionization of Helium in Strong Laser Fields," *Phys. Rev. Lett.* **84**, 443-446 (2000).
11. R. Moshhammer, B. Feuerstein, W. Schmitt, A. Dorn, C. D. Schröter, J. Ullrich, H. Rottke, C. Trump, M. Wittmann, G. Korn, K. Hoffmann, and W. Sandner, "Momentum Distributions of Ne^{7+} Ions Created by an Intense Ultrashort Laser Pulse," *Phys. Rev. Lett.* **84**, 447-450 (2000).
12. A. Rudenko, K. Zrost, B. Feuerstein, V. L. B. de Jesus, C. D. Schröter, R. Moshhammer, and J. Ullrich, "Correlated Multielectron Dynamics in Ultrafast Laser Pulse Interactions with Atoms," *Phys. Rev. Lett.* **93**, 253001 (2004).
13. P. B. Corkum, "Plasma perspective on strong field multiphoton ionization," *Phys. Rev. Lett.* **71**, 1994-1997 (1993).
14. Y. Liu, S. Tschuch, A. Rudenko, M. Dürr, M. Siegel, U. Morgner, R. Moshhammer, and J. Ullrich, "Strong-Field Double Ionization of Ar below the Recollision Threshold," *Phys. Rev. Lett.* **101**, 053001 (2008).
15. X. Liu, C. Figueira de Morisson Faria, W. Becker, and P.B. Corkum, "Attosecond electron thermalization by laser-driven electron recollision in atoms," *J. Phys. B* **39**, L305 (2006).
16. X. Liu, C. Figueira de Morisson Faria, and W. Becker, "Attosecond electron thermalization in laser-induced nonsequential multiple ionization: hard versus glancing collisions," *New J. Phys.* **10**, 025010 (2008).
17. Q. Li, Y. Zhou and P. Lu, "Universal time delay in the recollision impact ionization pathway of strong-field nonsequential double ionization," *J. Phys. B* **50**, 225601 (2017).
18. J. Ullrich, R. Moshhammer, A. Dorn, R. Dörner, L.P.H. Schmidt, and H. Schmidt-Böcking, "Recoil-ion and electron momentum spectroscopy: Reaction-microscopes," *Rep. Prog. Phys.* **66**, 1463 (2003).
19. O. Jagutzki, A. Cerezo, A. Czasch, R. Dörner, M. Hattas, M. Huang, V. Mergel, U. Spillmann, K. Ullmann-Pfeffer, T. Weber, H. Schmidt-Böcking, and G. D. W. Smith, "Multiple hit readout of a microchannel plate detector with a three-layer delay-line anode," *IEEE T Nucl. Sci.* **49**, 2477-2483 (2002).
20. H. Kang, K. Henrichs, M. Kunitski, Y. Wang, X. Hao, K. Fehre, A. Czasch, S. Eckart, L. Ph. H. Schmidt, M. Schöffler, T. Jahnke, X. Liu, and R. Dörner, "Timing Recollision in Nonsequential Double Ionization by Intense Elliptically Polarized Laser Pulses," *Phys. Rev. Lett.* **120**, 223204 (2018).
21. H. Kang, K. Henrichs, Y. Wang, X. Hao, S. Eckart, M. Kunitski, M. Schöffler, T. Jahnke, X. Liu, and R. Dörner, "Double ionization of neon in elliptically polarized femtosecond laser fields," *Phys. Rev. A* **97**, 063403 (2018).
22. A. S. Alnaser, X. M. Tong, T. Osipov, S. Voss, C. M. Maharjan, B. Shan, Z. Chang, and C.L. Cocke, "Laser-peak-intensity calibration using recoil-ion momentum imaging," *Phys. Rev. A* **70**, 023413 (2004).
23. J. S. Parker, B. J. S. Doherty, K. T. Taylor, K. D. Schultz, C. I. Blaga, and L. F. DiMauro, "High-Energy Cutoff in the Spectrum of Strong-Field Nonsequential Double Ionization," *Phys. Rev. Lett.* **96**, 133001 (2006).
24. S. X. Hu, "Optimizing the FEDVR-TDCC code for exploring the quantum dynamics of two-electron systems in intense laser pulses," *Phys. Rev. E* **81**, 056705 (2010).
25. R. Panfili, J. H. Eberly and S. L. Haan, "Comparing classical and quantum dynamics of strong-field double ionization," *Opt. Express* **8**, 431-435(2001).
26. R. Panfili, S. L. Haan and J. H. Eberly, "Slow-Down Collisions and Nonsequential Double Ionization in Classical Simulations," *Phys. Rev. Lett.* **89**, 130011(2002).
27. D. F. Ye, X. Liu, and J. Liu, "Classical Trajectory Diagnosis of a Fingerlike Pattern in the Correlated Electron Momentum Distribution in Strong Field Double Ionization of Helium," *Phys. Rev. Lett.* **101**, 233003 (2008).
28. Y. Zhou, Q. Liao, and P. Lu, "Asymmetric electron energy sharing in strong-field double ionization of helium," *Phys. Rev. A* **82**, 053402 (2010).
29. Y. Zhou, C. Huang, A. Tong, Q. Liao, and P. Lu, "Correlated electron dynamics in nonsequential double ionization by orthogonal two-color laser pulses," *Opt. Express* **19**, 2301-2308 (2011)
30. L. Zhang, X. Xie, S. Roither, Y. Zhou, P. Lu, D. Kartashov, M. Schöffler, D. Shafir, P. Corkum, A. Baltuska, A. Staudte, M. Kitzler, "Subcycle Control of Electron-Electron Correlation in Double Ionization," *Phys. Rev. Lett.* **112**, 193002 (2014).

31. G. L. Yudin and M. Y. Ivanov, "Nonadiabatic tunnel ionization: Looking inside a laser cycle," *Phys. Rev. A* **64**, 013409 (2001).
32. N. B. Delone and V. P. Krainov, "Energy and angular electron spectra for the tunnel ionization of atoms by strong low-frequency radiation," *J. Opt. Soc. Am. B* **8**, 1207-1211 (1991).
33. N. I. Shvetsov-Shilovski, S. P. Goreslavski, S. V. Popruzhenko, and W. Becker, "Ellipticity effects and the contributions of long orbits in nonsequential double ionization of atoms," *Phys. Rev. A* **77**, 063405 (2008).
34. M. Y. Wu, Y. L. Wang, X. J. Liu, W. D. Li, X. L. Hao, and J. Chen, "Coulomb-potential effects in nonsequential double ionization under elliptical polarization," *Phys. Rev. A* **87**, 013431 (2013).
35. Y. Li, B. Yu, Q. Tang, X. Wang, D. Hua, A. Tong, C. Jiang, G. Ge, Y. Li, and J. Wan, "Transition of recollision trajectories from linear to elliptical polarization," *Opt. Express* **24**, 6469-6479 (2016)
36. X. Ma, Y. Zhou, and P. Lu, "Multiple recollisions in strong-field nonsequential double ionization," *Phys. Rev. A* **93**, 013425 (2016).
37. P. J. Ho, R. Panfili, S. L. Haan, and J. H. Eberly, "Nonsequential Double Ionization as a Completely Classical Photoelectric Effect," *Phys. Rev. Lett.* **94**, 093002 (2005).